

Triply differential cross-section measurements in the double photoionization of D_2 and He with asymmetric kinematic conditions

S. A. Collins,¹ A. Huetz,² T. J. Reddish,¹ D. P. Secombe,¹ and K. Soejima³

¹*Physics Department, Newcastle University, Newcastle-upon-Tyne, NE1 7RU, United Kingdom*

²*Laboratoire de Spectroscopie Atomique et Ionique, Université Paris-Sud, Bâtiment 350, 91405, Orsay Cedex, France*

³*Graduate School of Science and Technology, Niigata University, Niigata-shi 950-21, Japan*

(Received 23 January 2001; published 14 November 2001)

The breakup of D_2 following the absorption of a single photon, leading to four free charged particles interacting via the Coulomb force, has been investigated. Triply differential cross sections (TDCSs) of the two ejected electrons were measured for selected asymmetric kinematic conditions, namely, a 20 eV electron in coincidence with a 5 eV “reference” electron fixed at four different angles. The results are compared with helium TDCSs and, although the respective angular distributions have similar features, there are surprising differences that could have their origin in two-center interference effects.

DOI: 10.1103/PhysRevA.64.062706

PACS number(s): 33.80.Eh, 32.80.Fb

During the last decade there have been a variety of photoelectron-photoelectron coincidence, or $(\gamma, 2e)$, studies of direct photodouble ionization (PDI) in helium to determine mutual angular distributions of the two ejected electrons (for a recent review see [1]). These $(\gamma, 2e)$ “triply differential cross section” (TDCS or $\sigma^{(3)}$) measurements are a sensitive probe of electron correlation and, therefore, are of considerable importance as they provide a stringent test for emerging theories [e.g., Refs. [2–9]]. Helium, the simplest two-electron system, is ideal for such studies since double-ionization results in free electrons and a nucleus, which all interact via the long-range Coulomb force. This process is now well understood in helium and the shapes and magnitudes of calculated TDCSs are generally in good agreement with the experimental measurements [1]. Interest has recently turned to similar studies on H_2/D_2 , the most fundamental two-electron molecule. The first $(\gamma, 2e)$ angular-distribution measurements in D_2 [10] were obtained with equal energy electrons, $E_1 = E_2 = 10$ eV, at a photon energy ($h\nu$) of 71.1 eV and revealed a heliumlike two-lobe structure. These results were later confirmed [11,12] and subsequent theoretical studies [13–18] have established the selection rules and highlighted the respective kinematic conditions for atomlike and true molecular behavior.

Apart from the initial electron-electron coincidence studies mentioned above, the only other experimental work probing PDI in H_2 , or the isoelectronic D_2 , is that of Dorner *et al.* [19], who measured electron-ion coincidences at a lower photon energy (58 eV), and by Dujardin *et al.* [20] and Kossmann *et al.* [21] who made pioneering ion-ion coincidence measurements. The scarcity of experimental data is primarily due to the purely repulsive nature of the upper state and the broad Franck-Condon “overlap” that distributes the PDI cross section over a large range of possible electron and ion energies. This, together with a relatively low total PDI cross section (σ^{2+}), which peaks at $\sim 0.5 \times 10^{-20} \text{ cm}^2$ at ~ 70 eV where $\sigma^{2+}/\sigma^+ \sim 3\text{--}4\%$, results in a very low coincidence count rate and makes the experiments extremely challenging. Improvement of the detection efficiency of this weak process requires the collection of electrons over a wide

(θ, ϕ) angular range. This can be achieved using toroidal analyzers, which are simultaneously angle- and energy-dispersive; these have already been applied to this problem for both atoms and molecules with considerable success [10–11,22–24]. An alternative approach, with even greater potential, is to detect the electrons over 4π sr using time-of-flight “momentum-mapping” techniques [25–27].

Here we report the first $(\gamma, 2e)D_2$ TDCSs measured using an asymmetric ($E_1 \neq E_2$) electron energy sharing condition. Moreover, the emission direction (θ_1) of the “reference” electron (whose energy is E_1), with respect to the electric field ($\hat{\epsilon}$), was chosen to be small. These two conditions have been shown to be the most physically interesting in the case of helium at energies significantly above the double-ionization threshold. As will be discussed later, the ungerade component’s contribution to the TDCS is most evident when $\theta_1 = 0^\circ$ and is enhanced further by increasing the electron energy asymmetry (E_2/E_1) [22]. Unfortunately, however, at this angular condition the TDCS yield is at its lowest and the measurement of the lower-energy electron is inevitably hindered by background signals arising indirectly from single-ionization processes (i.e., photoelectrons from H_2^+ scatter off metal surfaces and liberate low-energy electrons.) The TDCSs were measured at $h\nu = 104$ eV (He) and 76.1 eV (D_2), corresponding to an excess energy, E , of 25 eV. Our electron energies were selected for maximum asymmetry within the discussed constraints, i.e., the choice of the slower electron energy E_1 being limited by noise, and E by the overall cross section. Consequently, this experiment was considerably more difficult than the previous studies using the same apparatus [10,11], where the two electron energies were equal and θ_1 was in general much larger than 0° . It should also be noted that measurement of TDCSs at $\theta_1 \rightarrow 0^\circ$ using the momentum mapping techniques mentioned above is also very difficult due to the vanishing detection solid angle.

The experiments were performed on the SU6 undulator beamline at the Super-ACO synchrotron (France) using an angle-resolved spectrometer based on a toroidal geometry [28]. The photon beam, having a polarization state given by

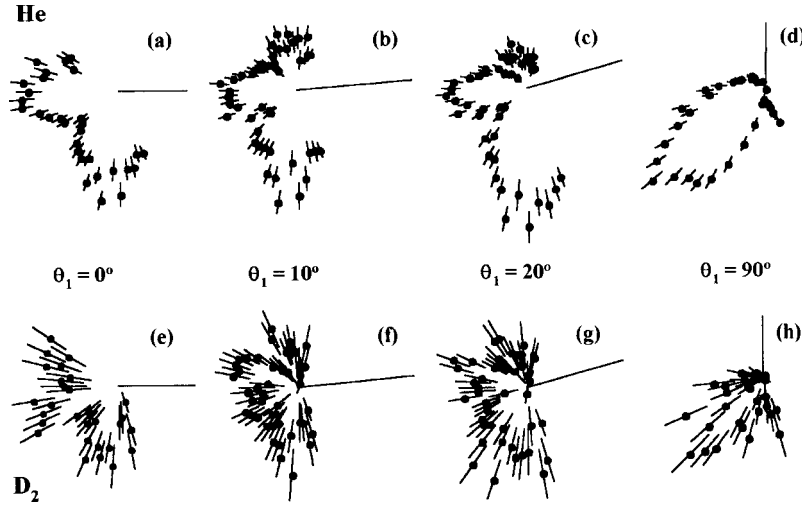


FIG. 1. $(\gamma, 2e)$ triply differential cross sections for He and D_2 with $S_1 = 0.9 \pm 0.05$, $S_3 = 0$. The reference electron has an energy (E_1) of 5 eV and E_2 is 20 eV, in all cases the data points are plotted in 5° intervals and each plot is on an arbitrary scale. The spectra with $\theta_1 = 0^\circ (\pm 20^\circ), 10^\circ (\pm 10^\circ), 20^\circ (\pm 10^\circ)$ are from coincidence measurements between the two toroidal analyzers. The latter two plots contain reflected information from $\theta_1 = -10^\circ$ and -20° using a procedure described in Ref. [24] that utilizes the symmetry about the electric field vector. The scatter is generally greatest at $\theta_2 \sim 270^\circ$ due to a minimum in the argon spectrum used for normalization. The $\theta_1 = 90^\circ (\pm 7^\circ)$ plots are taken from the coincidence measurements between the large toroidal and cylindrical analyzers.

the Stokes parameters, $S_1 = 0.90 \pm 0.05$ and $S_2 = S_3 = 0$, and an energy resolution of ≈ 400 meV at 75 eV, was merged with a coaxial effusive gas jet of conical geometry. Photoelectrons emitted in the plane orthogonal to the photon beam direction were energy analyzed by one 127° cylindrical and two toroidal analyzers. The smaller of the two toroidal analyzers and the 127° analyzer were both tuned to detect 5 eV electrons (E_1), with energy resolutions of ≈ 300 meV and ≈ 600 meV, respectively, and the larger toroid to detect 20 eV electrons (E_2) with ≈ 650 meV resolution. The larger toroid has an angular range corresponding to $145^\circ \leq \theta_2 \leq 290^\circ$ and the smaller toroidal analyzer has a 60° range that allows one to select θ_1 values centred at $-20^\circ (340^\circ) \rightarrow 20^\circ$, in 10° intervals. The “out-of-plane” angular acceptance for both toroidal analyzers is $\approx \pm 9^\circ$. The 127° analyzer has a fixed angular position of $\theta_1 = 90^\circ$ with an angular acceptance of $\approx \pm 7^\circ$. Coincidences between the two toroidal analyzers were recorded concurrently with those between the large toroidal and cylindrical analyzers.

As in earlier studies, D_2 was used in preference to H_2 because of gas-flow properties that result in a higher number density in the interaction region. TDCSs were measured for both D_2 and He using the same spectrometer tuning conditions, enabling a direct comparison of the two results. Since helium is relatively well studied, the He results provide a suitable frame of reference against which similarities and differences in the measured TDCS features can be evaluated. In each case the experiment was limited not by photon flux but by the ratio of “true-to-random” coincidences, which was measured to be $\sim 2:1$ (He) and $\sim 1:1$ (D_2) between the two toroidal analyzers. Due to the relatively small number of PDI events, the random counts are predominantly caused by coincidences between noise signals. The corresponding “true” coincidence count rates (integrated over all detection angles) were ~ 150 and ~ 20 events/h for helium and D_2

respectively, and about an order of magnitude lower for the other ($127^\circ + \text{large toroid}$) coincidence spectrum that had a “true-to-random” ratio of $\sim 5:1$. The random coincidences were statistically removed in the data processing (described in Ref. [28]) using standard procedures [29]. The angular response of the two toroidal analyzers needs to be calibrated against a known mutual angular distribution. Therefore, we measured mutual angular distributions between a 6.2 eV Auger electron and a 20 eV photoelectron in Ar ($h\nu = 71.31$ eV), which can be obtained with high statistical accuracy; the small change in E_1 (5 eV \rightarrow 6.2 eV) will not significantly alter the measured angular distribution. Although this process has not been previously investigated for these kinematic conditions, such distributions arising from two-step PDI are known to have reflection symmetry about $\theta_2 = 180^\circ$ and 90° for $\theta_1 = 0^\circ$ [e.g., [30]] and this property has been used in determining the normalization function.

The measured TDCSs for D_2 and He are shown in Fig. 1 and each distribution has been corrected with the same normalization function. The helium data are in excellent agreement [31] with “hyperspherical R matrix with semiclassical outgoing waves” (HRM-SOW) calculations [9]; the details of the calculation and further comparisons between theory and experiment will be discussed elsewhere [32]. This agreement indicates that, for D_2 , the possible systematic errors arising from the normalization method are negligible in comparison to the random errors. The two $\theta_1 = 90^\circ$ spectra [Figs. 1(d) and 1(h)] are quite similar. Both targets exhibit a pronounced minimum for back-to-back emission and, despite the poor statistics, the detected D_2 lobe appears to peak at a slightly larger mutual angle ($\theta_{12} \approx 138 \pm 5^\circ$) than in the He case ($\theta_{12} \approx 132 \pm 2^\circ$), as in earlier equal-energy studies [10–12]. In the $\theta_1 = 0^\circ$ orientation—where physically the TDCS has reflection symmetry about the $\hat{\epsilon}$ axis—the He TDCS

profile exhibits the classic three-lobe structure [Fig. 1(a)]. This reflection symmetry is also present in the case of D_2 , provided there is no selection of the molecular orientation—as in this study. Although there are similarities between the $\theta_1=0^\circ$ He and D_2 spectra [Figs. 1(a) and 1(e)], in D_2 , the lobe centered around $\theta_2=180^\circ$ not only has a relatively larger yield compared to the “lower” lobe—but is separated by a deeper minimum—but it is significantly broader with a slight minimum at $\sim\theta_2=180^\circ$. This minimum has been quantified by determining the following ratio for D_2 and He:

$$[\sigma^{(3)}(\theta_2 \sim 150^\circ) + \sigma^{(3)}(\theta_2 \sim 210^\circ)]/2[\sigma^{(3)}(\theta_2 \sim 180^\circ)],$$

yielding 1.3 ± 0.4 and 0.7 ± 0.1 , respectively. As in He, there is a rapid evolution in the shape of the TDCS as θ_1 departs from 0° [see Figs. 1(b), 1(c), 1(f), and 1(g)] and there are strong similarities in the TDCS features for the two targets. For example, the relative intensities of the “lower” and “upper” lobes (at $\theta_2 \sim 270^\circ, \sim 90^\circ$) increase and decrease with θ_1 , respectively.

To provide insight into the origin of the above features, Feagin [13,14] developed an appropriate He-like expression for the TDCS with arbitrary electron-pair energy sharing. This expression can be integrated over all molecular orientations for comparison with this study. This approach relies on the dominance ($\sim 96\%$) of $^1S^e$ character in a single-center expansion of the H_2 ground-state wave function. The TDCS depends on amplitudes, denoted by Σ and Π , corresponding to excitation that is parallel and perpendicular to the molecular axis, together with angular factors depending on the directions of the electrons (\hat{k}_1, \hat{k}_2) and electric field vector ($\hat{\epsilon}$). Expressing the formula in terms of widely-used gerade (a_Σ^g, a_Π^g) and ungerade (a_Σ^u, a_Π^u) amplitudes, that are symmetric and antisymmetric, respectively, for the interchange of the two electrons [2,22], one obtains

$$\begin{aligned} \sigma^{(3)}[D_2] = & \frac{2}{15} |a_\Sigma^g(\hat{\epsilon} \cdot \hat{k}_1 + \hat{\epsilon} \cdot \hat{k}_2) + a_\Sigma^u(\hat{\epsilon} \cdot \hat{k}_1 - \hat{\epsilon} \cdot \hat{k}_2)|^2 \\ & + \frac{7}{15} |a_\Pi^g(\hat{\epsilon} \cdot \hat{k}_1 + \hat{\epsilon} \cdot \hat{k}_2) + a_\Pi^u(\hat{\epsilon} \cdot \hat{k}_1 - \hat{\epsilon} \cdot \hat{k}_2)|^2 \\ & + \frac{6}{15} \text{Re}[(a_\Sigma^g)^*(\hat{\epsilon} \cdot \hat{k}_1 + \hat{\epsilon} \cdot \hat{k}_2) + (a_\Sigma^u)^* \\ & \times (\hat{\epsilon} \cdot \hat{k}_1 - \hat{\epsilon} \cdot \hat{k}_2))(a_\Pi^g(\hat{\epsilon} \cdot \hat{k}_1 + \hat{\epsilon} \cdot \hat{k}_2) \\ & + a_\Pi^u(\hat{\epsilon} \cdot \hat{k}_1 - \hat{\epsilon} \cdot \hat{k}_2))] + \frac{1}{15} |(a_\Sigma^g - a_\Pi^g) \\ & \times (\hat{k}_1 + \hat{k}_2) + (a_\Sigma^u - a_\Pi^u)(\hat{k}_1 - \hat{k}_2)|^2, \end{aligned} \quad (1)$$

where the $a_{\Sigma,\Pi}^g$ and $a_{\Sigma,\Pi}^u$ amplitudes depend on E_1, E_2 , and the mutual angle θ_{12} . This expression is valid for 100% linearly polarized light (i.e., $S_1=1$ —and can be easily adapted for $S_1<1$) and it reduces to the more familiar helium form when $a_\Sigma^g \rightarrow a_\Pi^g$, $a_\Sigma^u \rightarrow a_\Pi^u$, giving

$$\sigma^{(3)}[\text{He}] = |a^g(\hat{\epsilon} \cdot \hat{k}_1 + \hat{\epsilon} \cdot \hat{k}_2) + a^u(\hat{\epsilon} \cdot \hat{k}_1 - \hat{\epsilon} \cdot \hat{k}_2)|^2. \quad (2)$$

The first three terms in Eq. (1) have similar angular behavior to helium, but the fourth—or molecular—term depends only on the mutual angle between the two electrons (θ_{12}) and not their angles with respect to the electric field vector. This significant difference has important implications for the selection rules and, consequently, the relative sizes of the observed lobes in comparison to helium (see Ref. [14] for a full discussion of the $E_1=E_2$ case). The forms of Eqs. (1) and (2) show the importance of the $\hat{k}_1 = -\hat{k}_2$ direction. When $\theta_1=90^\circ$ there is a node in the TDCS for both He and D_2 for equal energy sharing (i.e., when the ungerade amplitudes are necessarily zero). This selection rule is still valid for He in the case of asymmetric energies but only holds in D_2 if $a_\Sigma^u = a_\Pi^u$. The observed minimum [Fig. 1(h)] suggests that the magnitudes of these two amplitudes are not too dissimilar. In order to *estimate* the widths of the observed lobes for $\theta_1=90^\circ$ one can make the following approximations, namely: (a) any molecular differences are small, i.e., $a_\Sigma^g \approx a_\Pi^g$ and $a_\Sigma^u \approx a_\Pi^u$, and (b) that $a^g > a^u$ for this energy sharing. Given that a^g can be well-represented by a Gaussian function centered at $\theta_{12}=180^\circ$ [1], one can use the Levenberg-Marquardt algorithm to fit the resulting expression for the TDCS to the data and so obtain the half widths Γ of $|a_g|^2$. This results in $\Gamma = 92 \pm 2^\circ$ and $79 \pm 5^\circ$ for He and D_2 , respectively, which is in keeping with the corresponding 91° and 78° Γ values obtained for the $E_1=E_2$ condition at the slightly lower 20 eV excess energy [11].

Considering now the $\hat{k}_1 = -\hat{k}_2$ direction when $\theta_1=0^\circ$, the TDCS is only sensitive to the a^u amplitudes for both targets. But even here the TDCS is more complicated in D_2 as the yield depends on *both* the amplitude and phase differences between the a_Σ^u and a_Π^u amplitudes. Clearly, detailed knowledge of the functional forms of all four amplitudes and their relative phases is required to obtain the general TDCS shape. In helium, the three-lobe structure can be obtained by using Gaussian functions as approximations to the two amplitudes, together with a phase factor [33]. If one adopts this approach for the four D_2 amplitudes in Eq. (1), one will still obtain a symmetric three-lobe structure for $\theta_1=0^\circ$. Thus the apparent four-lobe structure [Fig. 1(e)] in the D_2 TDCS would require the mutual angle dependence of the ungerade amplitudes to be significantly different from a Gaussian.

A further possibility is that the differences in the TDCS structure are a result of interference arising from the two-center nature of PDI in diatomic molecules. Walter and Briggs [15] showed that this effect gives rise to an additional mutual angle term in the TDCS for the simplest case, where one treats the final state as the product of plane waves. This term depends on the electrons' relative momentum vector ($\mathbf{k}_- = (\mathbf{k}_1 - \mathbf{k}_2)/2$), the size of the internuclear separation (R) and the angle between \mathbf{k}_- and the molecular axis. Although this interference behavior is predicted to be most evident for molecules whose axes are all orientated in a single direction (“fixed in space”), the effect would still be discernible when integrated over all molecular orientations, as in the case of this experiment, resulting in the following expression:

$$\frac{\partial^2 \sigma}{\partial k_1 \partial k_2} \propto [k_1(\hat{\epsilon} \cdot \hat{k}_1) + k_2(\hat{\epsilon} \cdot \hat{k}_2)]^2 \left[1 + \frac{\sin(2k_- R)}{2k_- R} \right]. \quad (3)$$

While this relation has the same nodal structure as in the He TDCS (2), due to the first factor, the second, θ_{12} -dependent “molecular factor” $[F(\theta_{12})]$ can have a minimum at $\theta_{12} = 180^\circ$ depending on the E_1 and E_2 values. For this interference effect to be observed $k_- > 1/2R \sim 0.34$ a.u. The maximum value of k_- in this experiment is 0.909 a.u. which is just high enough to satisfy this condition, and with our kinematics ($E_1 = 5$ eV, $E_2 = 20$ eV) the molecular factor in Eq. (3) indeed exhibits a shallow minimum at $\theta_{12} = 180^\circ$ [$(F(180^\circ)/F(0^\circ) \approx 0.6)$]. In a more realistic model including Coulomb interactions between the four particles, this effect could be larger because, at this photon energy, the internuclear axes are not isotropically distributed at the instant of dissociation, but exhibit a strong preference perpendicular to the polarization direction, quantified by a large and negative ion—asymmetry parameter ($\beta \approx -0.7$) [21]. Moreover, these interference effects may become most visible when θ_1 is close to 0° , as the antiparallel emission of the two electrons is then mostly orthogonal to the nuclear axis, i.e., in the middle of the two ion centers. The shallow minima around $\theta_{12} = 180^\circ$ in Fig. 1(e) and Fig. 1(f) are in qualitative agreement with this simplified picture. Even assuming the Born-

Oppenheimer approximation, an accurate determination of this effect will also require integration over the Franck-Condon width corresponding to our energy resolutions. Nevertheless, we have demonstrated that the observed perturbations from He-like TDCS expectations are not inconsistent with anticipated two-center interference behavior.

These experimental observations and qualitative explanations urgently require further theoretical investigation. The scatter associated with the data points is large and further ($\gamma, 2e$) measurements are needed at this and other asymmetric kinematic conditions. PDI studies using “fixed-in-space” molecules would be significantly more sensitive to these molecular effects and the authors are aware of preliminary attempts to perform these measurements [34]. The present study has shown that the similarities between the helium and D_2 TDCSs observed in equal-energy-sharing conditions survive in unequal-sharing conditions. It has also highlighted interesting differences that have yet to be fully understood in this most fundamental molecule.

This work was done with financial assistance from EPSRC and the EU Large Scale Facilities Program. D.P.S. and S.A.C. gratefully acknowledge EPSRC for their funding. We would like to thank A. Dickinson for his critical reading of the manuscript, and P. Selles and L. Malegat for providing He TDCS calculations.

-
- [1] J. S. Briggs and V. Schmidt, *J. Phys. B* **33**, R1 (2000).
 - [2] A. Huetz *et al.*, *J. Phys. B* **24**, 1917 (1991).
 - [3] F. Maulbetsch and J. S. Briggs, *J. Phys. B* **26**, 1679 (1993).
 - [4] A. K. Kazansky and V. N. Ostrovsky, *J. Phys. B* **27**, 447 (1994).
 - [5] M. Pont and R. Shakeshaft, *Phys. Rev. A* **51**, R2676 (1995).
 - [6] A. S. Kheifets and I. Bray, *J. Phys. B* **31**, L447 (1998).
 - [7] T. N. Rescigno *et al.*, *Phys. Rev. A* **57**, 318 (1999).
 - [8] M. S. Pindzola and F. Robicheaux, *Phys. Rev. A* **61**, 052707 (2000).
 - [9] L. Malegat, P. Selles, and A. K. Kazansky, *Phys. Rev. Lett.* **85**, 4450 (2000).
 - [10] T. J. Reddish *et al.*, *Phys. Rev. Lett.* **79**, 2438 (1997).
 - [11] J. P. Wightman, S. Cvejanović, and T. J. Reddish, *J. Phys. B* **31**, 1753 (1998).
 - [12] N. Scherer, H. Lörch, and V. Schmidt, *J. Phys. B* **31**, L817 (1998).
 - [13] J. M. Feagin, *J. Phys. B* **31**, L729 (1998).
 - [14] T. J. Reddish and J. M. Feagin, *J. Phys. B* **32**, 2473 (1999).
 - [15] M. Walter and J. S. Briggs, *J. Phys. B* **32**, 2487 (1999).
 - [16] M. Walter and J. S. Briggs, *Phys. Rev. Lett.* **85**, 1630 (2000).
 - [17] M. Walter, J. S. Briggs, and J. M. Feagin, *J. Phys. B* **33**, 2907 (2000).
 - [18] S. Sen and N. Chandra, *Phys. Rev. A* **62**, 052702 (2000).
 - [19] R. Dörner *et al.*, *Phys. Rev. Lett.* **81**, 5776 (1998).
 - [20] G. Dujardin *et al.*, *Phys. Rev. A* **35**, 5012 (1987).
 - [21] H. Kossmann *et al.*, *Phys. Rev. Lett.* **63**, 2040 (1989).
 - [22] P. Lablanquie *et al.*, *Phys. Rev. Lett.* **74**, 2192 (1995).
 - [23] J. Mazeau *et al.*, *J. Phys. B* **30**, L293 (1997).
 - [24] S. Cvejanović *et al.*, *J. Phys. B* **33**, 265 (2000).
 - [25] H. Bräuning *et al.*, *J. Phys. B* **31**, 5149 (1998).
 - [26] R. Dörner *et al.*, *Phys. Rev. A* **57**, 1074 (1998).
 - [27] A. Huetz and J. Mazeau, *Phys. Rev. Lett.* **85**, 530 (2000).
 - [28] T. J. Reddish *et al.*, *Rev. Sci. Instrum.* **68**, 2685 (1997).
 - [29] I. E. McCarthy and E. Weigold, *Phys. Rep.* **27**, 275 (1976).
 - [30] B. Krassig, O. Schwarzkopf, and V. Schmidt, *J. Phys. B* **26**, 2589 (1993).
 - [31] P. Selles and L. Malegat (private communication).
 - [32] P. Selles, L. Malegat, and A. K. Kazansky (unpublished).
 - [33] S. Cvejanović and T. J. Reddish, *J. Phys. B* **33**, 4691 (2000).
 - [34] R. Dörner (private communication).